A simple model for control of COVID-19 infections on an urban campus

Robert A. Brown[a,1]

[a]College of Engineering, Boston University, Boston, MA 02215

Contributed by Robert A. Brown, June 26, 2021 (sent for review March 19, 2021; reviewed by James J. Collins and Michael J. Mina)

A customized susceptible, exposed, infected, and recovered compartmental model is presented for describing the control of asymptomatic spread of COVID-19 infections on a residential, urban college campus embedded in a large urban community by using public health protocols, founded on surveillance testing, contact tracing, isolation, and quarantine. Analysis in the limit of low infection rates—a necessary condition for successful operation of the campus—yields expressions for controlling the infection and understanding the dynamics of infection spread. The number of expected cases on campus is proportional to the exogenous infection rate in the community and is decreased by more frequent testing and effective contact tracing. Simple expressions are presented for the dynamics of superspreader events and the impact of partial vaccination. The model results compare well with residential data from Boston University's undergraduate population for fall 2020.

COVID-19 | infection modeling | surveillance testing

The COVID-19 pandemic has challenged residential colleges and universities to design and implement layers of public health protocols to repopulate residential campuses and restore in-person learning. Developing these protocols is especially challenging for urban campuses where students, faculty, and staff are in constant contact with a larger community. Students living on and off campus are constantly interacting with city residents and students from other institutions. Control of viral spread in this environment requires limiting the number of on-campus cases to prevent rapid spread of the disease among student populations living in congregate housing.

The challenge is made much more complex with COVID-19 because, as documented by others (1, 2), a significant fraction of the infected people may be asymptomatic during all or a portion of the time when they can infect others. The analysis presented here is based on the hypothesis that control of COVID-19 infection rates on a college campus requires frequent surveillance testing of students, staff, and faculty, coupled with isolation of positive cases and contact tracing and quarantining of close contacts.

A simple mathematical framework is developed for describing the dynamics of infection in a university community with a surveillance testing system. The model assumes that the university is embedded in a larger urban area so that there is exogenous transmission of the disease to members of the university community from people who are not in it. A customized version of the standard SEIR (susceptible, exposed, infected, and recovered) model (3) for infection spread is presented for this purpose. In the analysis, the exposed population corresponds to the asymptomatic carriers described above. The model demonstrates the usual range of dynamic response for a SEIR model, with high infection rates leading to herd immunity. The focus of our analysis is on control of the infection rate in the presence of exogeneous input from the surrounding community. It is demonstrated that this is possible in the linear response or asymptotic limit of low infection rate. In this limit, the spread of exogenously introduced infections decays exponentially in time, resulting in a bounded number of cases per day in proportion to the exogenous input. Over time, the total number of cases grows linearly if the daily exogenous input is constant. This linear regime has been observed in simulations by others (4), but its importance in the context described here has not been identified.

An asymptotic analysis valid in this limit is described that results in closed-form expressions for the control of the virus as a function of key parameters in the model, including the testing frequency and the test's sensitivity. The results complement numerical simulations using compartment (5) and network or agent-based models (4, 6) and have the advantage of simplicity. Finally, the predictions are discussed in the context of results from the residential undergraduate program at Boston University, where such a surveillance system using qRT-PCR and contacting tracing was implemented during fall 2020 (7).

Results

Modified SEIR Model. The modified SEIR model is shown in Fig. 1 and was inspired by a presentation by Hosoi who first proposed it to model COVID-19 transmission (8). Beginning with N members, the susceptible population $S(t)$ becomes infected either from transmission within the university from either an asymptomatic and infectious member $A(t)$ or an infectious and symptomatic member $I(t)$, both at an infection rate β (the rate of infection per person per unit time). The disease can also be acquired outside the community, as represented by the rate of exogeneous cases $E(t)$ introduced per day per member. Asymptomatic individuals $A(t)$ are assumed to either become infectious $I(t)$ at the rate f_S or recover $R(t)$ at the rate f_R. Symptomatic individuals are identified and moved to quarantine $Q(t)$ (quarantine in this model accounts for both isolation and quarantine in practice) at the rate f_Q and recover at the rate f_R.

Surveillance testing at a frequency f_T is incorporated by moving asymptomatic individuals to quarantine with an efficiency of s. We model a test such as qRT-PCR, neglecting the low false-positive rate and assuming that there is a negligible time lag between the time of the test and the result. A turnaround for the test of under a day suffices for this assumption to be valid. The COVID-19 infection rate in a university community is modeled by

Significance

A simple model shows that control of COVID-19 infection driven by asymptomatic transmission on an urban, residential college campus is possible by instituting comprehensive public health protocols founded on surveillance testing and contact tracing. The model gives expressions for the number of infections expected as a function of these protocols and compares well with data from a large residential university for fall 2020.

Author contributions: R.A.B. performed research and wrote the paper.

Reviewers: J.J.C., Massachusetts Institute of Technology; and M.J.M., Harvard T.H. Chan School of Public Health.

The author declares no competing interest.

[1]Email: rabrown@bu.edu.

Published September 2, 2021.

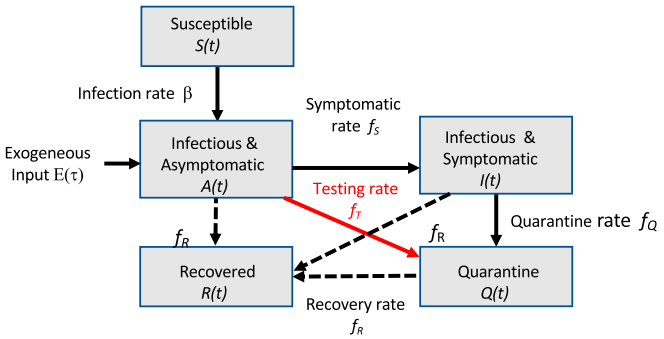

Fig. 1. Schematic of modified SEIR model showing each population and the rates for moving between each population. The impact of testing is shown in red.

estimating the recovery rate $f_R \equiv 1/T_R$, where T_R is an estimate for the time course of the disease. The rate of conversion of asymptomatic to symptomatic cases is modeled as $S_s f_R$, where S_s is the fraction of infections that become symptomatic within time T_R. The large-scale study from South Korea (9) puts the asymptomatic fraction between 0.55 and 0.7, depending on age, while Oran and Topol (2) estimate it at 0.4.

The differential equations that govern this model are

$$\frac{dS}{dt} = -\beta SA - \beta SI - ES \quad [1]$$

$$\frac{dA}{dt} = \beta SA + \beta SI - f_S A - f_R A - sf_T A + ES \quad [2]$$

$$\frac{dI}{dt} = f_S A - f_R I - f_Q I \quad [3]$$

$$\frac{dQ}{dt} = f_Q I + sf_T A - f_R Q \quad [4]$$

$$\frac{dR}{dt} = f_R Q + f_R I + f_R A = f_R(Q + I + A). \quad [5]$$

Typically, this system of nonlinear, ordinary differential rate equations would be solved with an initial condition, such as taking all variables as zero at $t = 0$ at the start of the infection. An important feature of this model is that the university is modeled as a community immersed in a much larger urban environment with interactions between the two being accounted for through the "exogenous input" $E = E(t)$, which may vary in time. Then $NE(t)$ estimates the exogenous cases per day in the university and drives the infection rate in the university community. Without exogenous input—a cloistered university—an initial input of infections, $A(0) > 0$, would be needed to generate infections.

Rewriting Eqs. **1**–**5** in dimensionless form using N as the scale for populations and $(\beta N)^{-1}$ as the time scale introduces the reproduction number $R_o \equiv \beta N/f_R$ as the dimensionless parameter scaling the rate of disease transmission to recovery. The reproduction number is not an intrinsic property of the COVID-19 pathogen but a measure of the transmission of the disease within a specific setting and community. The parameter R_o is assumed to account for public health protocols such as social distancing, face covering, enhanced sanitation, and ventilation in the university. Paltiel et al. (5) suggest that values of R_o between 1.5 and 3.5 represent a reasonable range for modeling COVID-19 with these protocols, with larger values being appropriate when these protocols are relaxed. Alimohamadi et al. (10) applied meta-analysis to a number of previous reports and suggest that R_o for COVID-19 without mitigations is ~3.2, with 95% confidence that it is in the interval 2.81 to 3.82. Zhang et al. (11) suggest with 95% CI that R_o is in the range 2.06 to 2.52.

Modeling the behavior of college students with a simple value of R_o is an oversimplification. Students may adhere to the public health protocols (mask wearing and social distancing) while in classrooms, laboratories, and observed public settings on campus but then take much greater risks during small (and not so small) social gatherings on and off campus. The role of student behavior is discussed below.

A key feature of effective repopulation of the campus is the need to limit disease spread to low infection rates [$A(t) << N$] so that care of infected people and their close contacts is manageable by the university healthcare system and that the numbers do not overwhelm the housing set aside for quarantine and isolation. As shown in Fig. 2*A*, for a given constant daily rate of exogeneous cases numerical integration of the model, Eqs. **1**–**5**, and other models for COVID-19, exhibit three types of behavior, depending on the value of R_o: nonlinear response leading quickly in time to herd immunity (large infection rates) for high R_o, weakly nonlinear response leading to herd immunity over much longer long times at intermediate values of R_o, and what is referred to as "linear response" in which the infection rate remains low for very long times.

We focus on the linear behavior and approximate it by assuming that the number of infected individuals (and the number of exogeneous cases introduced) remains small over time compared to N. The analysis is performed rigorously by putting the model in dimensionless form and expanding the equations in this limit, with the further assumption that the number of exogeneous cases introduced each day is small compared to N, or $E(t) << 1$. The analysis is carried out in terms of dimensionless variables;

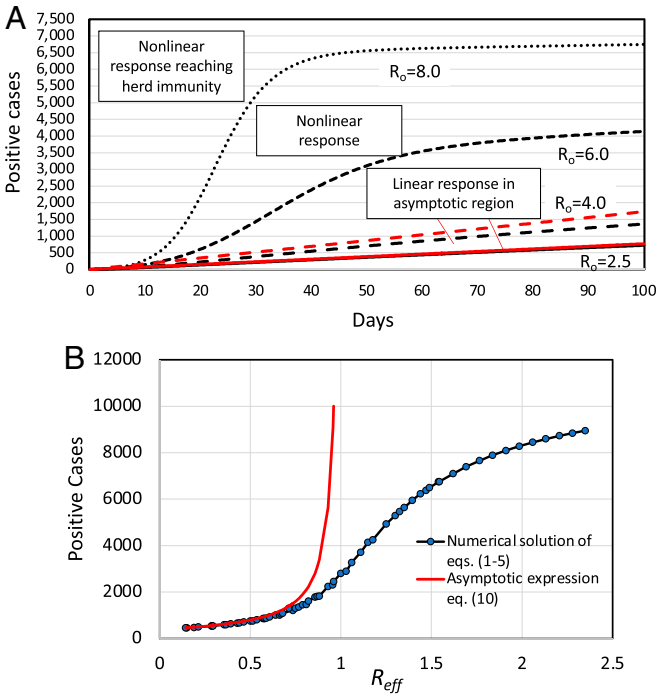

Fig. 2. Comparison of numerical result for the full model (without contact tracing), Eqs. **1**–**5**, with results from the asymptotic linear model. (*A*) Simulations for several values of R_o for 100 d for $f_T = \frac{2}{7}$ d^{-1} with other parameters fixed as described in the text. The model prediction from Eq. **10** is shown in red for the two values of R_o in the linear regime, $R_o = 4.0$ ($R_{eff} = 0.48$) and $R_o = 4.0$ ($R_{eff} = 0.77$). (*B*) Comparison of total number of positive cases predicted by numerical solution and by Eq. **10** shown in red.

however, all the results described below are presented in dimensional form so as to enhance their utility.

One further simplification is key to the analysis. It is assumed that symptomatic individuals $I(t)$ are moved to quarantine at a rate much faster than the rate of disease transmission, i.e., $f_Q \gg f_R$. This assumption essentially moves the burden of disease spread to the asymptomatic and infected population, $A(t)$, and is justified with rapid detection and isolation of symptomatic people. Making this assumption is mathematically equivalent to introducing the quasi-steady-state approximation (12) for $I(t)$, and gives the approximate expression

$$I(t) \cong \left(\frac{S_s f_R}{f_Q}\right) A(t) \ll A(t). \quad [6]$$

Hence, the infections caused by interactions with the symptomatic and infected population are small relative to those due to $A(t)$ and are neglected in the remainder of the analysis.

Under these assumptions, the remaining Eqs. **1**, **2**, **4**, and **5** decouple and the asymptomatic population $A(t)$ is governed by the simple linear differential equation written in dimensional form as

$$\frac{dA}{dt} = \frac{R_o}{T_R}\left(1 - \frac{1}{R_{eff}}\right) A(t) + NE_o p(t). \quad [7]$$

Here the exogeneous rate is expressed as $E(t) \equiv E_o p(t)$, where E_o is a constant and $p(t)$ is a dimensionless function of time; a constant exogeneous rate is expressed as $p(t) = 1$. The effective reproduction number R_{eff} in Eq. **7** is defined as

$$R_{eff} \equiv \frac{R_o}{\left(1 + S_s + sf_T T_R\right)}. \quad [8]$$

The expression for R_{eff} was derived by Hosoi (8) using a population balance on the asymptomatic cases. Three regions of behavior for $A(t)$ are identified, depending on whether R_{eff} is less than, equal to, or greater than 1. The region for stable (nonexponential) growth is

$$R_{eff} < 1. \quad [9]$$

For $R_{eff} > 1$, the model predicts exponential growth of $A(t)$ and the asymptotic approximations are invalid. When $R_{eff} < 1$ and without exogenous input [$p(t) = 0$], Eq. **7** always predicts an exponentially decreasing number of infections. This is the linear regime.

Constant Exogenous Rate. If the stability condition Eq. **9** holds, it is simple to solve Eq. **7** for a constant exogenous rate, i.e., $p(t) = 1$, to yield the steady-state result:

$$A(t) \equiv \frac{R_{eff}}{\left(1 - R_{eff}\right)} \frac{NE_o T_R}{R_o} = \frac{NE_o T_R}{\left(1 - R_{eff}\right)} \frac{1}{\left(1 + S_s + sf_T T_R\right)}. \quad [10]$$

Here $A(t)$ is a constant in time, proportional to the number of exogeneous cases introduced daily NE_o. Eq. **10** gives a useful estimate for the impact of surveillance testing; for a given R_o, increasing the testing frequency decreases R_{eff} and $A(t)$. The number of asymptomatic individuals is not observable (they are asymptomatic!). What is observable is the total of daily number of infected individuals detected either by testing or from symptoms. The expression for the number of detected cases per day is $C_T(t) \equiv (S_s + sf_T T_R)[A(t)/T_R]$. The total number of infections is computed as a function of time by solving for the difference $[N - S(t)]$ as

$$N - S(t) = \frac{NE_o T_R}{\left(1 - R_{eff}\right)} \frac{t}{T_R}, \quad [11]$$

which is the expression for linear (in time) growth of the number of infections. As shown in Fig. 2*A*, this expression is accurate for $R_{eff} < 1$. Interestingly, because the numerical results shown in Fig. 2*A* were computed with ranges of parameter values, the parameter R_{eff} also effectively parameterizes the model, Eqs. **1**–**5**, over the entire range of behavior. This scaling is rigorous justified as R_{eff} is the sole parameter in the dimensionless equations governing $A(t)$ and $S(t)$ in the limit where the quasi-steady-state approximation is valid.

How much testing is required to control the spread of the virus? For the parameter values listed below, here are examples: $f_T = \frac{1}{7}\,\mathrm{d}^{-1}$ gives $R_{eff} = \frac{Ro}{3.4}$, and $f_T = \frac{2}{7}\,\mathrm{d}^{-1}$ gives $R_{eff} = \frac{R_o}{5.2}$. Hence, surveillance testing twice per week will offset a transmission significantly rate higher than reported for COVID-19, $2.5 \le R_o \le 3.8$. If COVID-19 transmission is modeled with $R_o = 2.5$, then $R_{eff} = 0.48$ for $f_T = \frac{2}{7}\,\mathrm{d}^{-1}$. For a university community with $n = 10{,}000$ and a daily exogeneous rate of $NE_o = 4$ cases per day, the model predicts $A(t) = 20.7$ cases within the university community at any time and 6.2 cases per day detected. In a semester lasting 100 d, the model predicts 620 detected cases from 769 total infections (Eq. **11**).

Time-Varying Exogenous Rate. Eq. **7** is easily integrated for a variety of time-dependent inputs for $p(t)$ modeling the time variation of the exogenous rate. Polynomial expressions for $p(t)$ are especially simple to analyze. For example, linear growth in time for $p(t)$ results in linear growth of $A(t)$ and the total number of infections rising proportional to t^2. One of the most interesting cases is the effect of an event—sometimes referred to as a superspreader event—that is modeled as a pulse in exogenous cases at time $t = t_p$ using $p(t) = P_o \delta(t - t_p)$, where $\delta(t)$ is the Dirac delta function. It is straightforward to solve Eq. **7** to yield

$$A(t) \cong (P_o N) e^{\alpha \frac{(t - t_p)}{T_R}},\ t > t_p, \quad [12]$$

where $\alpha \equiv (R_{eff} - 1)(1 + S_s + sf_T T_R) < 0$ controls the rate of exponential decay of the pulse for $R_{eff} < 1$. A higher testing frequency increases α and speeds the decay of the pulse. For the parameters above $\alpha = -2.70$, so that a week after the event the pulse has decayed to $0.26 P_o N$. Under these conditions, only weak coupling exists between events (pulses) occurring one weekend and the next. Increasing the transmission rate (increasing R_o and R_{eff}) lengthens the time for pulse decay; for example, for $R_o = 3.8$, the pulse will decay only to $0.5 P_o N$ in a week and additive effects are expected from events on sequential weekends.

What can the model say about superspreader events affecting a campus? In the linear regime studied here, a large gathering causing a number of cases would be equivalent to a pulse input in the exogenous rate. The compartmental model treats these cases as spread about the entire university community, which is equivalent to each infected person dispersing into the community and potentially infecting others, according to the model. As long as $R_{eff} < 1$, the pulse of cases will decay in time according to the expression Eq. **12**. However, the more cases created by the pulse, the larger the demand for isolation and quarantine of students during the decay period. A mechanism for failure of the campus public health system is for demand to exceed the capacity of these special housing units.

Contact Tracing. Contact tracing is incorporated using a simple model that assumes that for every positive case identified, N_c close contacts are identified and a fraction σ of these develop the virus, hence they are from $A(t)$; then, $(1 - \sigma)$ is the fraction of the

contacts from $S(t)$. After quarantine, the close contacts are moved back to either the recovered or susceptible populations, depending on whether they have had the virus. Adding contact tracing to Eqs. **1**–**5** and applying the approximations described above leads to a delay differential Eqs. **13** and **14**:

$$\frac{dA}{dt} = \frac{R_o}{T_R}\left(1 - \frac{1}{R_{eff}}\right)A(t) + \frac{\sigma N_c}{T_R}\left(S_s + sf_T T_R\right)A(t - t_c) + NE_o p(t), \quad [13]$$

where t_c is the time lag between identifying the index case and moving the close contacts to quarantine. Eq. **13** has complicated solutions for arbitrary values of t_c (13, 14), including oscillations in time, if t_c is comparable to or greater than the time between tests. If t_c is small, that is, contact tracing is performed quickly compared to the testing cadence, Eq. **13** yields a result identical to Eq. **7** with R_{eff} replaced by

$$R_{eff}^{ct} \equiv \frac{R_o}{\left[\left(1 + S_s + sf_T T_R\right) + \sigma N_c\left(S_s + sf_T T_R\right)\right]}. \quad [14]$$

The additional infection control due to contact tracing is measured by comparing the expressions for R_{eff} and R_{eff}^{ct}. For $f_T = \frac{2}{7}\,\mathrm{d}^{-1}$, $N_c = 3$ and $\sigma = \frac{1}{6}$ (empirical values estimated from the Boston University data), $R_{eff}^{ct}/R_{eff} = 0.71$, or a 30% enhancement. By this result, increasing the testing frequency augments the effectiveness of contact tracing, if the number of infected close contacts σN_c remains constant. This may not be the case: More-frequent testing also decreases N_c, slowing disease spread. Conversely, less-frequent testing should lead to more close contacts and more disease spread.

Impact of Partial Vaccination. As the pandemic evolves vaccines become critical to restoring close-to-normal operation of a residential university. The analysis is expanded to include the effects of a partially effective vaccine in a partially vaccinated university community. We assume that the fraction of the community $f_v \equiv (1 - \varphi)$ has been vaccinated with a vaccine that has efficacy $e_v \equiv (1 - \epsilon)$; it is assumed that the transmission rate of the disease is lowered to $\epsilon\beta$ with vaccination. In the model the susceptible population is divided into unvaccinated φN and vaccinated $(1 - \varphi)N$ segments, each with the appropriate transmission rate. Repeating the analysis described above leads to the same expression for the rate equation for $A(t)$, Eq. **7**, with R_{eff} replaced by $R_{eff}^{v} \equiv \Phi R_{eff}$, where $\Phi \equiv \epsilon + \varphi(1 - \epsilon) \equiv (1 - e_v f_v)$. Operating in the linear or stable region requires $R_{eff}^{v} < 1$.

The relationship between vaccine efficacy and the vaccinated fraction of the population for a specific value of Φ is given by $\varphi = (\Phi - \epsilon)/(1 - \epsilon)$. Then, using no public health mitigations ($f_T = 0, N_c = 0, S_s = 0$) results in $R_{eff}^{v} = \Phi R_o$. Remaining in the linear region and living with the resulting higher transmission rates, perhaps $3 \le R_o \le 5$, will only be achievable with $\Phi < 0.2$, requiring highly effective vaccines and almost everyone vaccinated. Until herd immunity is achieved by a combination of vaccination and natural immunity, remaining in the linear regime may require some level of public health mitigations (e.g., mask wearing) and surveillance testing, especially in the congregate housing on a college campus.

Comparison with Boston University Data. The results described above assume that the infection rate from the surrounding community is constant in time. This was clearly not true during the fall of 2020 as urban universities operated in the midst of surging cases in their surrounding communities. The effect of the surge is investigated by comparing directly to data for Boston University's operation throughout fall 2020. The university operated during the fall (classes from 1 September 2020 to 10 December 2020, or 101 d) with a comprehensive qRT-PCR testing program for the entire campus community delivered by an on-campus testing laboratory. The protocol used by the university is described in ref. 7. The comparison here is for the undergraduate student population at Boston University during the fall, who were tested twice per week with a compliance rate of nearly 95%; test results were returned in an average of 18 h and students who tested positive were isolated. The average daily testing positivity rate for the semester was 0.2%. The contact tracing program resulted in close contacts being placed in quarantine in less than 12 h after identifying the index case. Examination of cases and close contacts showed almost no transmission of COVID-19 between the undergraduates and other campus populations and very low transmission in traditional classrooms and laboratories.

In the calculation, the exogenous rate $NE(t)$ is estimated using the daily rate of new infections reported in Suffolk County, MA (15) scaled for the ~10,000 student undergraduate population. The Suffolk County data are shown in Fig. 3 and demonstrate the rising infection rate throughout the fall caused by the second surge of infections seen across the country. Eq. **13** including contact tracing was numerically integrated with the Suffolk County data used for $p(t)$; the results are also shown in Fig. 3 and demonstrate how the model results qualitatively mirror the increasing infection rate in the county. This is not surprising. The timescale for change in the exogenous rate is somewhat slower than the fast timescale for the decay dynamics give in Eq. **13**. Under these conditions, a formal multiple timescale analysis (16) shows that the time-dependent response $A(t)$ approximately follows Eq. **10** with E_o replaced by $E_o p(t)$. The validity of this approximation depends on the separation of the timescales for

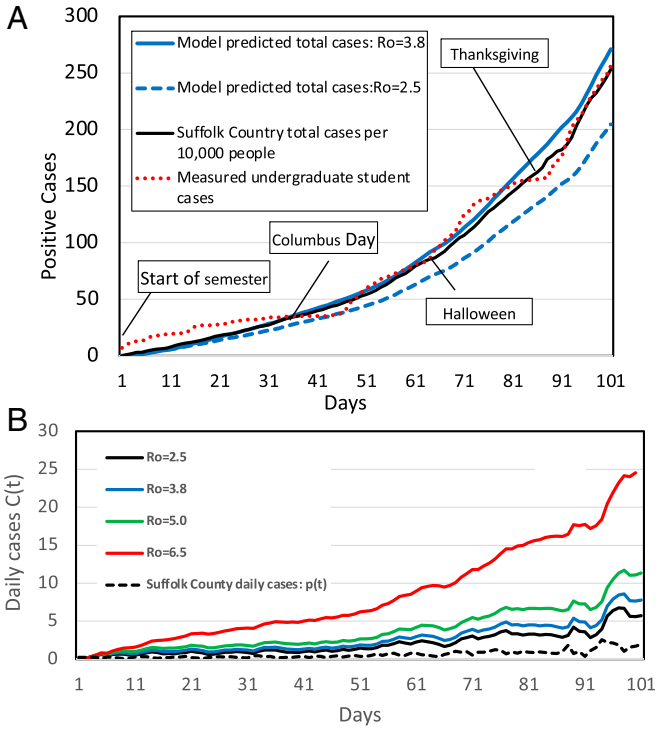

Fig. 3. Results for increasing exogenous input modeled by data from Suffolk County, MA compared to numerical solution of Eq. **7** and undergraduate positive cases at Boston University for fall semester (1 September 2020 to 10 December 2020). (*A*) Calculation of cumulative case are shown for both $R_o = 2.5$ and $R_o = 3.8$. (*B*) Calculation of the daily observed cases with R_o values of 2.5, 3.8, 5.0, and 6.5, corresponding to values of R_{eff}^{ct} of 0.34. 0.52, 0.68, and 0.89, respectively.

the decay of infections, given by Eq. **12** and the timescale for variation of $p(t)$.

The model calculations for the cumulative number of cases as shown in Fig. 3*A* for R_o values of 2.5 and 3.8 (spanning the range suggested in refs. 5 and 10) to highlight the sensitivity of the model to this variable. We have not attempted to "fit" the model to specific parameter values. If we did, the sensitivity to other variables, such as the duration of the infection period T_R, the efficiency of the PCR testing s, and the fraction of asymptomatic infections that become symptomatic S_s should also be considered. We expect such a fitting process to be sensitive to the value selected for T_R. Varying T_R from 14 d (the value used in our calculations) to 10 d (holding R_o constant) decreases R_{eff} by ∼21%.

Also, as recognized by King et al. (17), accurate parametric fitting of the model to the data is better based on prediction of the number of daily cases, not the cumulative number of cases as shown in Fig. 3, and by implementing a stochastic variant of the model. This approach has not been pursued, as the focus of this study is on the simplicity of the results described here.

The number of daily cases $C_T(t)$ is shown in Fig. 3*B* for a range of values of R_o. Note that $C_T(t)$ remains relatively small throughout the semester, ranging for $R_o = 2.5$ from none at the start of the semester to 28 on day 95 at the height of the pulse caused by Thanksgiving gatherings. Increasing R_o increases the daily cases but does not appreciably change the response time to variations in $p(t)$.

The cumulative infections seen in the Boston University undergraduate population during the semester are shown in Fig. 3*A*. The comparison between the model and the case data is better than expected, especially with no attempt to fit the model parameters to the data. The comparison does suggest that the transmission on campus is better modeled by the higher reproduction number $R_o = 3.8$ for the values of the parameters used in these calculations.

Can the case data from Boston University be explained without considering exogenous input? The data are not described with $p(t) = 0$ if $R_{eff} < 1$. Then, Eq. **7** predicts exponential decay of the on-campus infections for all reasonable values of R_o and the disappearance of the disease, which is not what was observed.

The student data also show surges of cases in time that are loosely coupled to events during the semester when compliance with social distancing and mask wearing were known to be laxer or when travel from campus (Thanksgiving week) introduced additional risk. These events cause dynamics in the viral transmission rate that cannot be captured by this simple model. However, the analysis for the response to a pulse suggests that the impact of such events decays if they are adequately separated in time.

Discussion

Urban universities are integrated within their local communities, with their students, staff, and faculty potentially bringing infections to the campus. The model gives a simple description for the interplay of the COVID-19 transmission rate with surveillance testing and contact tracing to keep the infection rate in the linear regime. The simple compartment model cannot capture the details of behavior that impact the transmission rate, such as mask wearing, social distancing, ventilation, and sanitation. In our description these effects are lumped into the value used for the reproduction number R_o.

Capturing the behavior of college students with a single constant is probably impossible. Although students may comply with protocols in formal campus settings, their behavior in social gatherings is more likely to mimic the higher values of R_o associated with the viral spread. This behavior could be responsible for the better fit of the model with the data in Fig. 3 using $R_o = 3.8$.

Successful operation of the campus is contingent on the success of testing and contact tracing and on the logistics for quarantine. For a constant exogenous rate, the model predicts a steady-state need for quarantine spaces as $Q(t) = (1 + N_c)(S_s + sf_T T_R)A(t)$, where the expression for $A(t)$ is given by Eq. **7**. For the parameters used in the example above $Q(t) = 274$ spaces, or equivalent to under 3% of the population.

The effectiveness of surveillance testing also is predicated on the specificity of the testing method; false-positive results can easily swamp the capacity of the quarantine system. For 10,000 students tested twice per week, a false positivity rate of only 1% would lead to over 400 students per day (false positives and their close contacts) mistakenly placed in quarantine, unless secondary testing is used to sort out the false positives. The positivity rate was ∼0.2% for the Boston University testing program in fall 2020 and has decreased substantially as vaccinations have become available.

The applicability of the simple model presented here to a residential university or any residential community hinges on the speed of delivery of testing and contact tracing, as well as the compliance of community members with the protocols for quarantine, isolation, and symptom attestation. At Boston University PCR tests were returned in an average of 18 h and contact tracing and quarantining of individuals was completed in under 12 h. As discussed above for contact tracing, delays in execution of these steps leads to nonlinear behavior; Eq. **13** becomes a delay differential equation. Oscillations in time for $A(t)$ can result, which would be difficult to assess and complicate control strategies.

Boston University developed robust systems for symptom attestation, contact tracing, isolation, quarantine, and communication strategies for each of these efforts (7). Our success with controlling virus spread was a result of the compliance of community members with these protocols.

Materials and Methods

The numerical integrations of Eqs. **1**–**5** used to produce Fig. 1 and of Eq. **7** used in Fig. 3 were carried out using a simple Euler method written by the author. Parameter values used in all calculations for the customized SEIR model were as follows: test efficiency (accounting for test sensitivity, indeterminate tests [less than 0.2% in Boston University experience], and students who miss their tests) $s = 0.9$; fraction of asymptomatic infections that convert to symptomatic. $S_s = 0.6$, consistent with the data presented in ref. 3. The duration of the infectious period is taken as $T_R = 14$ d. This estimate is in rough agreement with estimates in Larremore et al. (6) for the time of high viral load for an infected person.

Data Availability. All study data are included in the article and/or supporting information. Previously published data were used for this work (7).

ACKNOWLEDGMENTS. I am grateful for the assistance of L. Decarie with compiling the data from the Boston University Community testing program and the data from Suffolk County, MA.

1. H. Nishiura *et al*., Estimation of the asymptomatic ratio of novel coronavirus infections (COVID-19). *Int. J. Infect. Dis.* **94**, 154–155 (2020).
2. D. P. Oran, E. J. Topol, Prevalence of asymptomatic SARS-CoV-2 infections. *Ann. Intern. Med.* **173**, 363–367 (2020).
3. M. Martcheva, *An Introduction to Mathematical Epidemiology* (Springer, 2010).
4. A. Nishi *et al*., Network interventions for managing the COVID-19 pandemic and sustaining economy. *Proc. Natl. Acad. Sci. U.S.A.* **117**, 30285–30294 (2020).
5. A. D. Paltiel, A. Zheng, R. P. Walensky, Assessment of SARS-CoV-2 screening strategies to permit safe reopening of college campuses in the United States. *JAMA Netw. Open* **3**, e2016818 (2020).
6. D. B. Larremore *et al*., Test sensitivity is secondary to frequency and turnaround time for COVID-19 frequency. *Sci. Advances* **7**, eabd5393 (2021).
7. D. H. Hamer *et al*., Control of COVID-19 transmission on an urban university campus during a second wave of the pandemic. *medRxiv* [Preprint] (2021). https://doi.org/10.1101/2021.02.23.21252319 (Accessed 26 February 2021).
8. M. Dahleh, P. Hosoi, D. Jones, Rules of thumb for reopening. https://idss.mit.edu/vignette/rules-of-thumb-for-reopening/. Accessed 4 June 2020.
9. C.-Y. Jung *et al*., Clinical characteristics of asymptomatic patients with COVID-19: A nationwide cohort study in South Korea. *Int. J. Infect. Dis.* **99**, 266–268 (2020).

10. Y. Alimohamadi, M. Taghdir, M. Sepandi, Estimate of the basic reproduction number for COVID-19: A systematic review and meta-analysis. *J. Prev. Med. Public Health* **53**, 151–157 (2020).
11. S. Zhang *et al*., Estimation of the reproduction number of novel coronavirus (COVID-19) and the probable outbreak size on the Diamond Princess cruise ship: A data-driven analysis. *Int. J. Infect. Dis.* **93**, 201–204 (2020).
12. L. A. Segel, M. Slemrod, The quasi-steady-state assumption: A case study in perturbation. *SIAM Rev.* **31**, 446–477 (1989).
13. H. Gorecki, S. Fuksa, P. Grabowski, A. Korytowski, *Analysis and Synthesis of Time Delay Systems* (John Wiley and Sons, Warzawa, 1989).
14. F. M. Asi, A. G. Ulsoy, Analysis of a system of linear delay differential equations. *J. Dyn. Syst. Meas. Control* **125**, 215–223 (2003).
15. Commonwealth of Massachusetts, COVID-19 raw data, March 1, 2021. https://www.mass.gov/doc/covid-19-raw-data-march-1-2021/download. Accessed 14 January 2020.
16. A. H. Nayfeh, *Perturbation Methods* (John Wiley and Sons, 1973).
17. A. A. King, M. Domenech de Cellès, F. M. G. Magpantay, P. Rohani, Avoidable errors in the modelling of outbreaks of emerging pathogens, with special reference to Ebola. *Proc. R. Soc. Lond. B Biol. Sci.*, 10.1098/rspb.2015.0347 (2015).